Eco-friendly fabrication of PBDTTPD:PC71BM solar cells reaching a PCE of 3.8% using water-based nanoparticle dispersions

Peer-reviewed author version

D'OLIESLAEGER, Lien; PIROTTE, Geert; CARDINALETTI, Ilaria; D'HAEN, Jan; MANCA, Jean; VANDERZANDE, Dirk; MAES, Wouter & ETHIRAJAN, Anitha (2017)
Eco-friendly fabrication of PBDTTPD:PC71BM solar cells reaching a PCE of 3.8% using water-based nanoparticle dispersions. In: ORGANIC ELECTRONICS, 42, p. 42-46.

DOI: 10.1016/j.orge1.2016.12.018
Handle: http://hdl.handle.net/1942/23467

Eco-Friendly Fabrication of PBDTTPD:$PC_{71}BM$ Solar Cells Reaching a PCE of 3.8% Using Water-Based Nanoparticle Dispersions

Lien D'Olieslaeger,[a] Geert Pirotte,[b] Ilaria Cardinaletti,[a] Jan D'Haen,[a,c] Jean Manca,[d] Dirk Vanderzande,[b,c] Wouter Maes,[b,c] and Anitha Ethirajan*[a,c]

[a] UHasselt – Hasselt University, Institute for Materials Research (IMO-IMOMEC), Material Physics Division, Agoralaan, 3590 Diepenbeek, Belgium

[b] UHasselt – Hasselt University, Institute for Materials Research (IMO-IMOMEC), Design & Synthesis of Organic Semiconductors (DSOS) Agoralaan, 3590 Diepenbeek, Belgium

[c] IMEC, Associated lab IMOMEC, Wetenschapspark 1, 3590 Diepenbeek, Belgium

[d] UHasselt – Hasselt University, X-LaB, Agoralaan, 3590 Diepenbeek, Belgium

* Corresponding Author: anitha.ethirajan@uhasselt.be

Abstract

In this work we report on the eco-friendly processing of PBDTTPD:$PC_{71}BM$ organic solar cells using water-based nanoparticle (NP) dispersions. The polymer:fullerene NPs are prepared using the miniemulsion-solvent evaporation method, despite employing high-boiling solvents. Polymer solar cells are fabricated from these blend NPs and the device characteristics are studied in function of annealing time and temperature. The photoactive layer formation is carefully analyzed using atomic force microscopy (AFM). Annealing for longer times significantly increases the power conversion efficiency (PCE), up to 3.8%, the highest value reported for surfactant based NP solar cells. Our work shows that the low bandgap polymer PBDTTPD has the ability to afford reasonable efficiencies in NP solar cells in combination with $PC_{71}BM$ and paves the way to a truly eco-friendly processing of organic photovoltaics (OPVs).

Keywords: nanoparticles, polymer solar cells, low bandgap polymer, miniemulsion, eco-friendly processing

1. Introduction

In the last decade, organic solar cells have seen an increasing interest because they offer a suite of appealing properties, being light-weight, flexible, colorful, solution processable and applicable to large areas [1]. Donor-acceptor type low bandgap polymers (LBPs) with more efficient solar light harvesting capabilities have emerged as the most prominent electron donor materials in bulk heterojunction (BHJ) OPVs (in conjunction with fullerene acceptors) [2]. A plethora of such polymers have already been synthesized and applied in polymer solar cells, nowadays reaching PCEs beyond 11% [1, 3]. Among the high-efficiency polymers, PBDTTPD (poly[(benzo[1,2-

b:4,5-*b*']dithiophene)-*alt*-(4*H*-thieno[3,4-*c*]pyrrole-4,6(5*H*)-dione)]) - with 2-ethylhexyloxy and octyl side chains on the BDT and TPD units, respectively (see Figure 1) - is one of the most suitable materials toward upscaling. It has been demonstrated to give an average PCE of 7% [4,5,6], and we have recently reported an optimized continuous flow synthesis of this polymer, allowing reproducible large-scale production in a sustainable way [7]. PBDTTPD has also shown good thermo- and excellent photostability [4, 6]. Moreover, its 'synthetic complexity' versus efficiency ratio is close to the workhorse material P3HT [8].

One of the pivotal concerns of OPV technology is the need for hazardous organic solvents such as chloroform, chlorobenzene or *o*-dichlorobenzene to process the photoactive layer. Although greener solvents (such as xylene, anisol, …) are compelling alternatives [9,10,11], the solubility of the LBP is a limiting factor. In this aspect, water-based NP dispersions of the active layer materials, requiring only small amounts of halogenated solvents for particle formation, are obviously very attractive, as ultimately large area device fabrication using aqueous 'solar paint' is in all likelihood highly favored. Using this approach, the active layer morphology formation and deposition are separated into two different processes. Therefore, no organic solvents are required anymore for active layer deposition and large areas can be coated in an eco-friendly way. Furthermore, as the production of colloidal particles by solvent evaporation using a closed loop solvent extraction process is already in practice on an industrial scale, using the nanoparticle approach, the evaporated solvent can more easily be caught up and recovered than when using the traditional approach. Also, as the solid content of the dispersions can be easily tuned by concentrating or diluting the dispersion by addition or removal of water, large stocks of concentrated dispersions can be prepared at once and later diluted to the needed concentration and viscosity requirements for deposition of the active layer using different coating techniques [12] just before use. Such flexibility in large-scale fabrication of devices eases the hurdles in manufacturing with respect to health, environment and handling safety. Several research groups have synthesized NP dispersions for OPV devices, using the miniemulsion or the reprecipitation method, mainly employing P3HT and polyfluorenes, and more recently also a few LBP [13,14,15,16,17]. With the reprecipitation technique, wherein no surfactant is used, a maximum efficiency of 4% was reached using blend NPs consisting of P3HT and the fullerene acceptor ICBA [13]. For the surfactant based NPs, the reported maximum PCE is 2.6%, using the polymer donor P(TBT-DPP) and ICBA [16]. Usually low-boiling solvents have been used for NP formation. It is worth to note that, with solubility issues in low-boiling solvents, especially when increasing the molecular weight (MW), limited LBPs (mostly low MW) have been used for particle formation. In this regard, our group recently reported the synthesis of PCDTBT:$PC_{71}BM$ blend NPs employing a high MW polymer [18]. In this preceding work, the combined miniemulsion and emulsion/solvent evaporation technique developed by Kietzke *et al.* [14] was optimized for using *o*-dichlorobenzene (a high-boiling solvent) in the dispersed phase. Using these NPs, a PCDTBT:$PC_{71}BM$ solar cell with a top efficiency of 1.9% was fabricated [18].

Previously, with the in house synthesized PBDTTPD polymer, an excellent overall average PCE of 7.2% was obtained for standard BHJ OPV devices, which could even be improved to a record efficiency of 9.1% by using an ionic polythiophene-based cathodic interlayer [7]. In the present work, we have used this material to prepare PBDTTPD:$PC_{71}BM$ blend NPs by adapting our previously reported procedure combining the miniemulsion and the

emulsion/solvent evaporation technique (as PBDTTPD is a polymer with solubility issues and could not be dissolved in any of the low-boiling solvents).

2. Materials and methods

2.1 Materials

[6,6]-Phenyl-C_{71}-butyric acid methyl ester ($PC_{71}BM$; purity >99%) was obtained from Solenne. Chlorobenzene (purity >99%) was acquired from Sigma Aldrich and sodium dodecyl sulfate (SDS) from Merck. Zinc oxide (ZnO) nanoparticles were obtained from Nanograde and indium thin oxide (ITO) glass slides (20 Ω sq-1) from Kintec. The PBDTTPD polymer was prepared by Stille polycondensation in a continuous flow synthesis setup as reported previously [7].

2.2 PBDTTPD:$PC_{71}BM$ nanoparticle synthesis

PBDTTPD:$PC_{71}BM$ (1:1.5) blend NPs were prepared using the miniemulsion and emulsion/solvent evaporation technique. The donor polymer PBDTTPD (75 mg) and the fullerene acceptor $PC_{71}BM$ (112 mg) were dissolved in chlorobenzene (6 g) by magnetic stirring (500 rpm) at 80 °C in a nitrogen environment (total concentration 35 mg/mL). An aqueous phase consisting of SDS surfactant (37 mg; 0.4 wt%) in water (9 g) was added to this solution. After magnetic stirring at 1000 rpm for 1 h, the miniemulsion was obtained by ultrasonication for 180 s (30 s pulse, 20 s pause) at 60% amplitude using a Branson 450W digital sonifier (1/4" tip). The obtained miniemulsion was transferred to three round bottom flasks with a wide neck and left for 7 h at 60 °C (based upon full evaporation of a CB reference sample within 6 h and particle size evolution measured using dynamic light scattering after certain time intervals from a dispersion used as a control and treated identically to the sample). To compensate for the water loss during evaporation, additional water was added every hour to the miniemulsion. Excess surfactant was removed by multiple washing steps using Millipore membrane tubes (MWCO 30 kDa). The NPs were visualized using a Tecnai Spirit transmission electron microscope from FEI at an acceleration voltage of 120 keV. The hydrodynamic size was measured by dynamic light scattering using a Brookhaven Instruments Zetapals.

2.3 PBDTTPD:$PC_{71}BM$ NP device fabrication and characterization

Patterned ITO glass slides were cleaned with detergent, water, acetone and boiling isopropanol, and then treated with UV-ozone for 30 min. A ZnO nanoparticle layer was spincoated on top (0.1 wt% in isopropanol, 4000 rpm) and annealed at 150 °C for 10 min in a nitrogen atmosphere. Afterwards, the PBDTTPD:$PC_{71}BM$ (1:1.5) NP layer was deposited by spincoating of the NP dispersion (250 µL, 2000 rpm; 4% solid content). The layer was annealed in a nitrogen environment at different annealing temperatures to eliminate the residual water and to optimize film formation. The average thickness of the active layer of all devices ranged from 120 to 140 nm, as measured

by profilometry (DektakXT stylus profiler from Bruker). Finally, the substrates were transferred to a vacuum chamber to evaporate MoO_3/Al electrodes on top of the active layer (active area 0.03 cm²). The thickness of the MoO_3 and aluminum layers was measured to be 20 and 120 nm, respectively, using a quartz crystal monitor. All solar cells were characterized under AM1.5 illumination. The NP layer before and after annealing at different temperatures was imaged, in tapping mode, using a Bruker Multimode 8 atomic force microscope. Only the AFM images of the reference devices were corrected with a low band pass filter in order to remove streaks. The cross section of the device architecture was visualized using a Quanta 200FEG-SEM from FEI.

For the reference device fabrication, PBDTTPD (8 mg) and $PC_{71}BM$ (12 mg) were dissolved in a chlorobenzene:1-chloronaphthalene (95:5 vol%) solution or in pure chlorobenzene with a total concentration of 20 mg/mL. The solution was stirred overnight at 80 °C in a nitrogen atmosphere. The active layer was spincoated on top of the ZnO layer at a processing temperature of 115 °C. The average thickness of the active layer of all devices ranged from 90 to 110 nm, as measured by profilometry. To dry the active layer, the samples were placed in a vacuum chamber with a pressure of 5×10^{-7} mbar for 1.5 h. Afterwards, the MoO_3/Al top electrode was evaporated on top in the same way as for the NP devices.

3. Results and discussion

Blend NPs in a 1:1.5 PBDTTPD:$PC_{71}BM$ weight ratio were made using the procedure as visualized in Figure 1. As the highest device efficiencies reported in literature were achieved using chlorobenzene (CB) as the prime solvent [5], the latter was chosen here as the solvent for the dispersed phase. CB was evaporated at 60 °C and the loss of water during evaporation was compensated by adding water to the continuous phase. Although CB is still used for NP preparation, the quantity is approximately half of the amount generally used for spincoating the PBDTTPD:$PC_{71}BM$ active layer. A TEM image of the blend NPs is presented in Figure 1, visualizing the size and morphology. PBDTTPD and $PC_{71}BM$ are materials with similar TEM absorption contrast and therefore no phase separation can be observed. The average size of the particles was 32 nm, with a PDI of 0.108, as measured by dynamic light scattering. The average particle size from AFM (Figure 2A), measured through grain statistics using the Gwyddion software on a 1x1 µm² scan area, was approximately 35 nm. The solid content obtained after synthesis was around 0.4%, as additional water was added during NP fabrication.

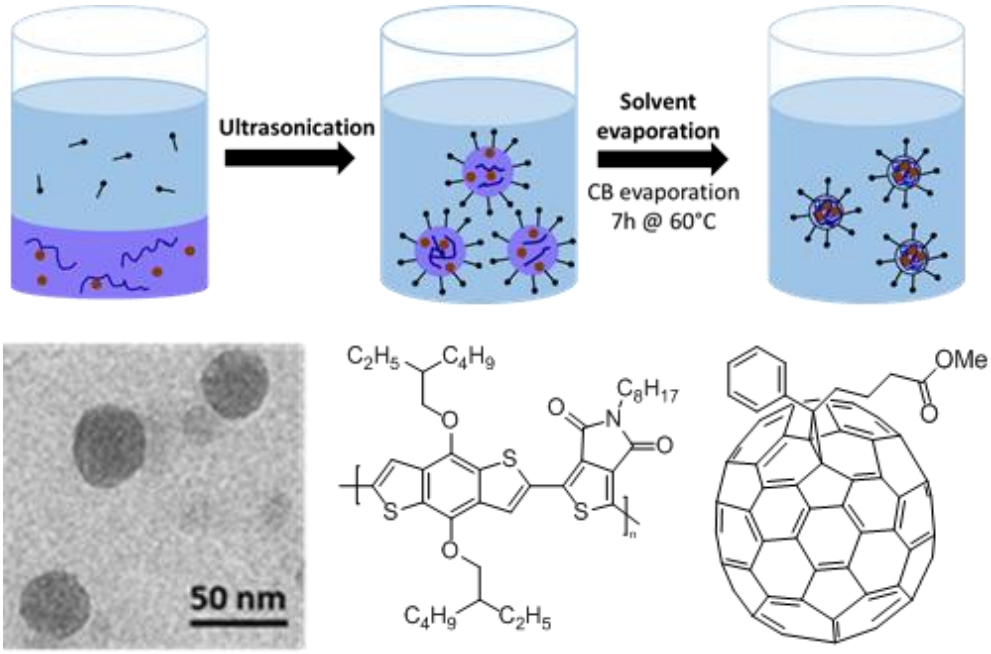

Figure 1. Schematic overview of the PBDTTPD:$PC_{71}BM$ NP preparation **(top)**, TEM image of the NPs **(bottom left)** and chemical structures of PBDTTPD **(bottom middle)** and $PC_{71}BM$ **(bottom right)**.

Polymer solar cells were then made out of the NP dispersions. As PEDOT:PSS is not compatible with spincoating of water-based dispersions, an inverted device architecture ITO/ZnO/PBDTTPD:$PC_{71}BM$/MoO_3/Al was used here. The active layer was deposited by spincoating the NP ink onto the ZnO layer. As can be seen from the AFM image in Figure 2(A), a nicely covered area of NPs was obtained. Afterwards, the layer was annealed at different temperatures to optimize active layer formation. Finally, MoO_3 and the top electrode were evaporated on top to finish the devices. In Figure 2(B), a cross-section back scattered electrons (BSE) - scanning electron microscope (SEM) image is shown to visualize the device built-up.

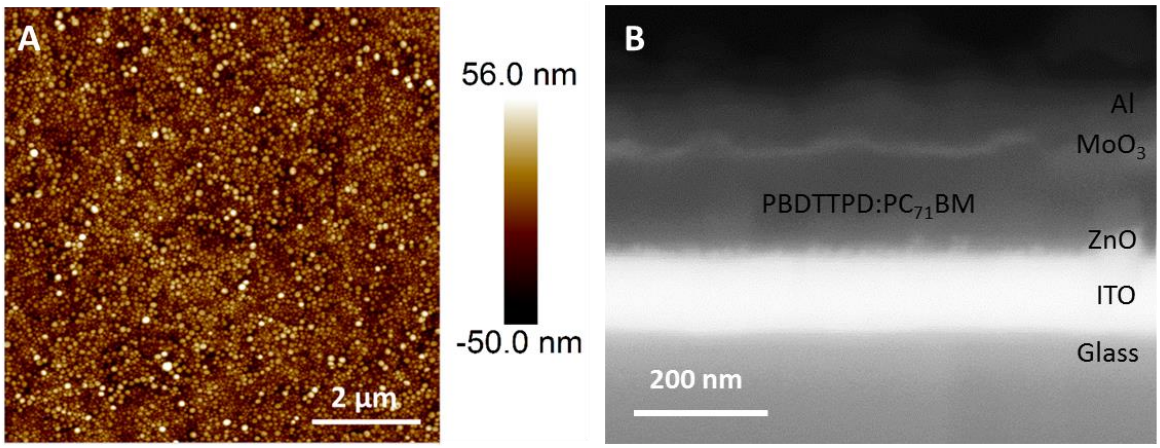

Figure 2. (A) AFM image showing the coverage of the PBDTTPD:$PC_{71}BM$ NP film after spincoating. **(B)** Cross-section BSE-SEM image of the best PBDTTPD:$PC_{71}BM$ NP solar cell (20 min annealing at 180 °C).

The device characteristics after annealing the NP films at different temperatures (for 4 min) are listed in Table 1. As PBDTTPD has a glass transition temperature of 143 °C (see Figure A1), an annealing temperature ranging from 150 to 200 °C was chosen. A clear rise in PCE from 0.3 to 2% can be seen when increasing the annealing temperature up to 180 °C. This trend is characterized by an increase in open-circuit voltage (V_{oc}; from 130 to 530 mV), short-circuit current density (J_{sc}; from 8.73 to 9.02 mA/cm²) and fill factor (FF; from 28 to 41%). Annealing at higher temperatures again lowers the PCE. The further rise in V_{oc} is overcompensated by the strong reduction in J_{sc}.

Table 1. *J-V* characteristics for the best PBDTTPD:$PC_{71}BM$ NP devices after thermal treatment at different temperatures and times (with the average values ± standard deviations over 4 devices in parentheses).

Thermal treatment	V_{oc} [mV]	J_{sc} [mA/cm²]	FF [%]	PCE [%]
150 °C – 4 min	130 (90±50)	8.73 (6.16±3.50)	28 (27±2)	0.3 (0.2±0.2)
160 °C – 4 min	240 (200±30)	9.13 (9.93±0.82)	32 (31±1)	0.7 (0.6±0.1)
170 °C – 4 min	430 (340±70)	9.53 (9.31±0.32)	38 (36±2)	1.6 (1.2±0.3)
180 °C – 4 min	**530 (500±30)**	**9.02 (8.75±0.59)**	**41 (40±1)**	**2 (1.8±0.2)**
190 °C – 4 min	600 (580±40)	7.53 (7.41±0.21)	40 (40±1)	1.8 (1.7±0.1)
200 °C – 4 min	630 (580±60)	6.87 (7.05±0.20)	39 (39±0)	1.7 (1.6±0.1)
180 °C – 20 min	**860 (764±136)**	**9.99 (10.45±0.64)**	**44 (40±6)**	**3.8 (3.2±0.8)**

In Figure 3, an AFM image of the NP layer before and after annealing at 180 °C is shown. After annealing, the layer is far from uniform yet and a particle-like morphology can still clearly be observed. The AFM images after annealing at different temperatures are all quite similar (see Figure A2), as expected from the comparable J_{sc} values obtained. The increase in V_{oc}, especially above 160 °C, could point to a better coverage of the substrate. This is also supported by the reduction of the leakage current for higher annealing temperatures, as suggested

by the dark current-voltage characteristics (presented in Figure A4). Although annealing at temperatures above 180 °C did not grant a homogeneous layer, the thermal treatment clearly promotes an overall smoothening of the film, which might result in an unfavorable compositional drift toward a less optimal morphology for higher temperatures (as further described in Appendix A).

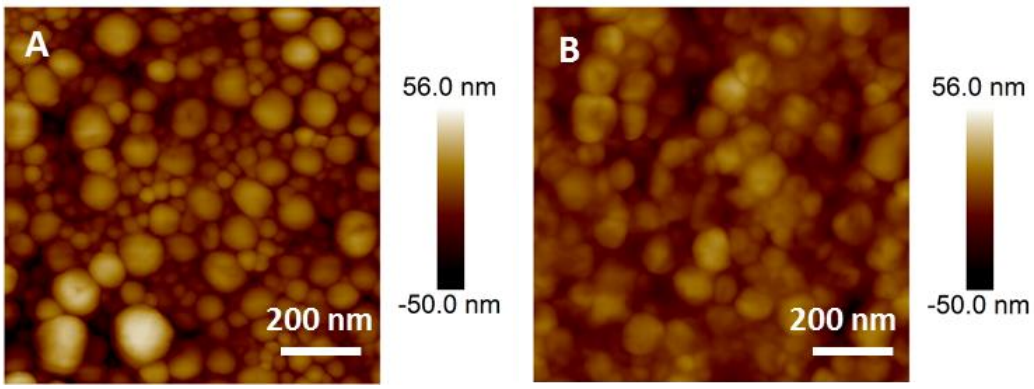

Figure 3. AFM image of a PBDTTPD:$PC_{71}BM$ NP film without annealing **(A)** and after annealing for 4 min at 180 °C **(B)**.

A longer annealing time was then applied to further improve the device characteristics. The NP layer was annealed for 20 minutes at 180 °C, which resulted in a strong efficiency increase to a maximum of 3.8% (V_{oc} = 860 mV, J_{sc} = 9.99 mA/cm², FF = 44%, 3.2 ± 0.8% average PCE; Table 1, Figure 4B). Mainly the V_{oc} increased substantially, with minor improvements in J_{sc} and FF as well. AFM analysis shows that the particle morphology is still recognizable, but the active layer is now smoother (Figure 4A), illustrating that annealing for a longer time further improves layer formation.

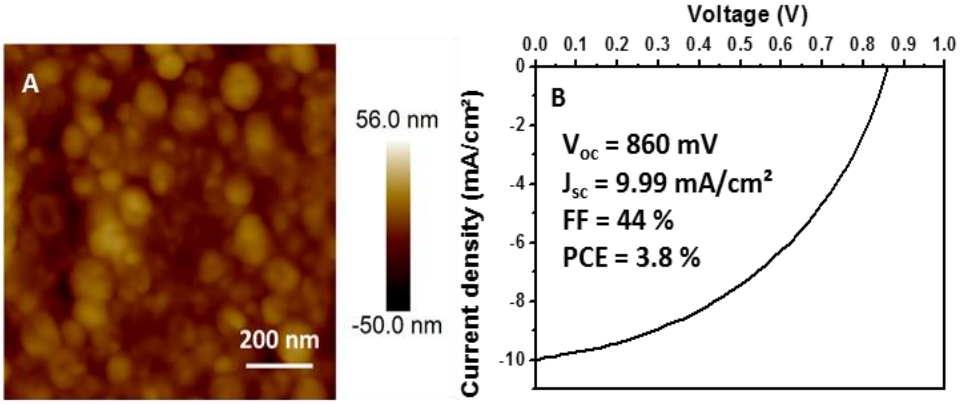

Figure 4. AFM image of the NP film (**A**) and *J-V* curve (**B**) for the best PBDTTPD:$PC_{71}BM$ NP solar cell after 20 min annealing at 180 °C.

To allow proper comparison, reference inverted polymer solar cells were made by spincoating the active layer materials from solution (see Table A1), using an optimal processing solvent mixture of CB and 1-chloronaphthalene (CN) (95:5) [5,19]. This resulted in a best PCE of 6.1% and an average PCE of 5.8 ± 0.4% (Table A1, Ref 1). A reference device was also made from pure CB solution, without the CN additive, affording a maximal

PCE of 3.9% (Table A1, Ref 2), very close to the best NP device. Furthermore, annealed reference devices were made without the additive, resulting in a best PCE of 4.3% when annealing at 180 °C for 4 minutes (Table A1, Ref 3) and 3.7% when annealing for 20 minutes (Table A1, Ref 4). Thermal annealing does not affect the efficiency significantly, whereas for the NP based solar cells, it is a necessary step toward layer formation. Nonetheless, the PCEs are very close when comparing the results without CN additive. AFM scans of the reference films show that the blends tend to assume a more fibrillary structure when deposited from pure CB solution (Figure A3), as opposed to the round features still visible for the (annealed) NP cast films. The characteristic shape of the latter might reflect the need to revise the (post)processing treatments to achieve optimal film formation.

4. Conclusions

To conclude, we have shown that PBDTTPD:$PC_{71}BM$ blend NPs can effectively be synthesized using the combination of miniemulsion and emulsion/solvent evaporation. As PBDTTPD is a material with solubility issues in standard low-boiling solvents, the NP preparation protocol was optimized for the use of chlorobenzene in the dispersed phase. Annealing the NP solar cells for 20 minutes at 180 °C afforded the best PCE of 3.8% and further improvements might be achievable by optimizing the film deposition and annealing protocol. These results definitely demonstrate the high potential of the NP approach for an eco-friendly preparation of organic solar cells and present an important leap forward toward affordable and highly effective solar paint [15].

5. References

[1] K. A. Mazzio, C. K. Luscombe, The future of organic photovoltaics. Chem. Soc. Rev. 44 (2015) 78-90.

[2] C. Liu, K. Wang, X. Gong, A. J. Heeger, Low bandgap semiconducting polymers for polymeric photovoltaics. Chem. Soc. Rev. 45 (2016) 4825-4846.

[3] J. Zhao, Y. Li, G. Yang, K. Jiang, H. Lin, H. Ade, W. Ma, H. Yan, Efficient organic solar cells processed from hydrocarbon solvents. Nat. Energy 1 (2016) 15027.

[4] J. A. Bartelt, J. D. Douglas, W. R. Mateker, A. E. Labban, C. J. Tassone, M. F. Toney, J. M. J. Fréchet, P. M. Beaujuge, M. D. McGehee, Controlling Solution-Phase Polymer Aggregation with Molecular Weight and Solvent Additives to Optimize Polymer-Fullerene Bulk Heterojunction Solar Cells. Adv. Energy Mater. 4 (2014) 1301733.

[5] C. Cabanetos, A. El Labban, J. A. Bartelt, J. D. Douglas, W. R. Mateker, J. M. J. Fréchet, M. D. McGehee, P. M. Beaujuge, Linear Side Chains in Benzo[1,2-*b*:4,5-*b*']dithiophene–Thieno[3,4-*c*]pyrrole-4,6-dione Polymers Direct Self-Assembly and Solar Cell Performance. J. Am. Chem. Soc. 135 (2013) 4656-4659.

[6] Y. Zou, A. Najari, P. Berrouard, S. Beaupré, B. Réda Aïch, Y. Tao, M. Leclerc, A Thieno[3,4-*c*]pyrrole-4,6-dione-Based Copolymer for Efficient Solar Cells. J. Am. Chem. Soc. 132 (2010) 5330-5331.

[7] G. Pirotte, J. Kesters, P. Verstappen, S. Govaerts, J. Manca, L. Lutsen, D. Vanderzande, W. Maes, Continuous Flow Polymer Synthesis toward Reproducible Large-Scale Production for Efficient Bulk Heterojunction Organic Solar Cells. ChemSusChem 8 (2015) 3228-3233.

[8] R. Po, G. Bianchi, C. Carbonera, A. Pellegrino, "All That Glisters Is Not Gold": an analysis of the synthetic complexity of efficient polymer donors for polymer solar cells. Macromolecules 48 (2015) 453-461.
[9] C. Sprau, F. Buss, M. Wagner, D. Landerer, M. Koppitz, A. Schulz, D. Bahro, W. Schabel, P. Scharfer, A. Colsmann, Highly efficient polymer solar cells cast from non-halogenated xylene/anisaldehyde solution. Energy Environ. Sci. 8 (2015) 2744-2752.
[10]) S. Li, H. Zhang, W. Zhao, L. Ye, H. Yao, B. Yang, S. Zhang, J. Hou, Green-Solvent-Processed All-Polymer Solar Cells Containing a Perylene Diimide-Based Acceptor with an Efficiency over 6.5%. Adv. Energy Mater. 6 (2016) 1501991.
[11] S. Zhang, L. Ye, H. Zhang, J. Hou, Green-solvent-processable organic solar cells. Mater. Today 19 (2016) 533-543.
[12] Y. Galagan, R. Andriessen (2012). Organic Photovoltaics: Technologies and Manufacturing, Third Generation Photovoltaics, V. Fthenakis (Ed.), ISBN: 978-953-51-0304-2, InTech.
[13] S. Gärtner, M. Christmann, S. Sankaran, H. Röhm, E.-M. Prinz, F. Penth, A. Pütz, A. E. Türeli, B. Penth, B. Baumstümmler, A. Colsmann, Eco-Friendly Fabrication of 4% Efficient Organic Solar Cells from Surfactant-Free P3HT:ICBA Nanoparticle Dispersions. Adv. Mater. 26 (2014) 6653-6657.
[14] T. Kietzke, D. Neher, M. Kumke, R. Montenegro, K. Landfester, U. Scherf, A Nanoparticle Approach To Control the Phase Separation in Polyfluorene Photovoltaic Devices. Macromolecules 37 (2004) 4882-4890.
[15] X. Zhou, W. Belcher, P. Dastoor, Solar Paint: From Synthesis to Printing. Polymers 6 (2014) 2832.
[16] N. A. D. Yamamoto, M. E. Payne, M. Koehler, A. Facchetti, L. S. Roman, A. C. Arias, Charge transport model for photovoltaic devices based on printed polymer:fullerene nanoparticles. Sol. Energy Mater. Sol. Cells 141 (2015) 171-177.
[17] N. P. Holmes, M. Marks, P. Kumar, R. Kroon, M. G. Barr, N. Nicolaidis, K. Feron, A. Pivrikas, A. Fahy, A. D. D. Z. Mendaza, A. L. D. Kilcoyne, C. Müller, X. Zhou, M. R. Andersson, P. C. Dastoor, W. J. Belcher, Nano-pathways: Bridging the divide between water-processable nanoparticulate and bulk heterojunction organic photovoltaics. Nano Energy 19 (2016) 495-510.
[18] L. D'Olieslaeger, M. Pfanmöller, E. Fron, I. Cardinaletti, M. Van Der Auweraer, G. Van Tendeloo, S. Bals, W. Maes, D. Vanderzande, J. Manca, A. Ethirajan, Tuning of PCDTBT:$PC_{71}BM$ blend nanoparticles for eco-friendly processing of polymer solar cells. Sol. Energy Mater. Sol. Cells. 159 (2017) 179-188.
[19] C. Dyer-Smith, I. A. Howard, C. Cabanetos, A. El Labban, P. M. Beaujuge, F. Laquai, Interplay Between Side Chain Pattern, Polymer Aggregation, and Charge Carrier Dynamics in PBDTTPD:PCBM Bulk-Heterojunction Solar Cells. Adv. Energy Mater. 5 (2015) 1401778.

Appendix A

Supporting information is available.

Acknowledgements

The authors wish to thank J. Kesters, J. Smits and H. Pellaers for technical support. A.E. is a post-doctoral fellow of the FWO.

Formatting of funding sources

The authors acknowledge financial support by Hasselt University (BOF), the Research Foundation – Flanders (FWO) (project G.0415.14N), and IAP 7/05 project FS2 (Functional Supramolecular systems), granted by the Science Policy Office of the Belgian Federal Government (BELSPO).